2022-04

Atmospheric transport of microplastics during a dust storm

Abbasi, S

10.1016/j.chemosphere.2021.133456
Chemosphere
Elsevier BV

Atmospheric transport of microplastics during a dust storm

Sajjad Abbasi [a,b] *, Mahrooz Rezaei [c,d], Farnaz Ahmadi [d], Andrew Turner [e]

[a] Department of Earth Sciences, College of Science, Shiraz University, Shiraz 71454, Iran

[b] Department of Radiochemistry and Environmental Chemistry, Faculty of Chemistry, Maria Curie-Skłodowska University, Lublin 20-031, Poland

[c] Meteorology and Air Quality Group, Wageningen University & Research, P.O. Box 47, 6700 AA Wageningen, the Netherlands

[d] Department of Soil Science, School of Agriculture, Shiraz University, Shiraz, Iran

[e] School of Geography, Earth and Environmental Sciences, University of Plymouth, PL4 8AA, UK

* Corresponding author. Department of Earth Sciences, College of Science, Shiraz University, 71454, Shiraz, Iran.

E-mail address: sajjad.abbasi.h@gmail.com; sajjad.abbasi@shirazu.ac.ir

https://doi.org/10.1016/j.chemosphere.2021.133456

Accepted 25 December 2021

Graphical Abstract

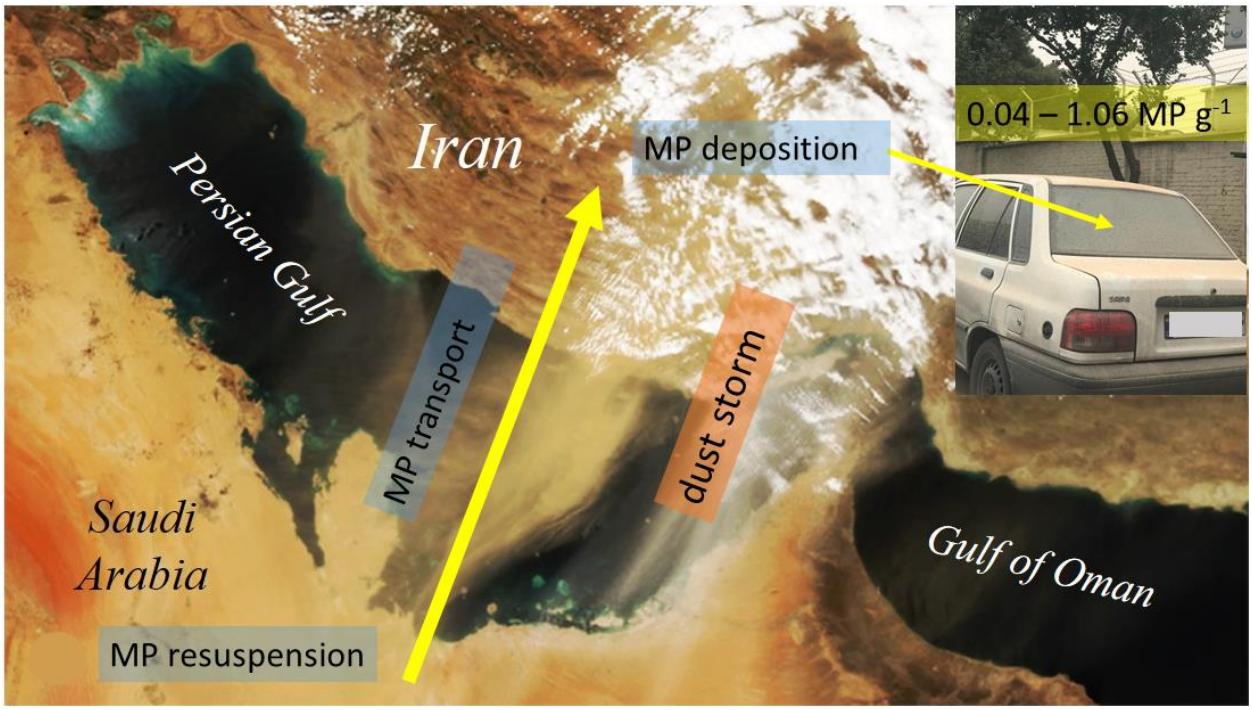

Abstract

Dust storms are common events in arid and semi-arid regions that have a wide range of impacts on the environment and human health. This study addresses the presence, characteristics and potential sources of microplastics (MPs) in such events by analysing MPs deposited with dust particles in the metropolis of Shiraz, southwest Iran, following an intense storm in May 2018. At 22 locations throughout the city, MP concentrations on a number basis ranged from 0.04 to 1.06 per g of dust (median = 0.31 MP g^{-1}). Particles were mainly fibrous, with a mean diameter of about 20 µm and > 50% under 100 µm in length, and polymer makeup was dominated by nylon, polypropylene and polyethylene terephthalate. Examination of selected MPs by scanning electron microscopy revealed varying degrees of weathering and contamination by extraneous geogenic particles amongst the samples. Using published MP concentrations in urban dusts and remote, arid soils, we estimate that between about 0.1 and 5% of MPs deposited by the dust storm are derived from local sources within the metropolis, with the remainder arising from more distant sources. HYSPLIT modelling, satellite imagery and published geochemical signatures of regional dust particles suggest that the deserts of Saudi Arabia constitute the principal distal and transboundary source. Dust storms may represent a significant means by which MPs are transported and redistributed in arid and semi-arid environments and an important source of MPs to the oceans.

Keywords: Microfibres; Weathering; Deposition; Source; Flux; Iran

1. Introduction

Dust storms are intense suspensions of geogenic silt- and clay-sized particulates that may last for several hours to several days. These events result from strong and turbulent winds acting on loose, sparsely vegetated soils and lithological units in arid and semi-arid regions, and in particular in inland drainage basins, and have the propensity to transport airborne particles over long distances (Tan et al., 2012; Srivastava et al., 2018; van der Does et al., 2018; Rashki et al., 2021). Dust storms have many and varied impacts on weather, climate and the environment. For example, high dust loadings may affect air temperature, cloud formation and convectional activity (including hurricane intensity) and are believed to play a major role in the delivery of iron and other nutrients to the oceans (Goudie, 2009). Dust storms also have significant adverse impacts on agriculture, urban infrastructure, solar power production, the economy, and human health and safety (Rashki et al., 2021). Regarding the latter, high loadings of suspended geogenic particles are directly responsible for transport accidents and respiratory complaints, cardiovascular diseases and other illnesses (Pauley et al., 1996; Tam et al., 2012), while the presence of associated materials or chemicals, like bioaerosols, heavy metals and radionuclides, may pose additional allergenic or chronic health risks (Ogorodnikov, 2011; Behrooz et al., 2020; Soleimani et al., 2020).

In the recent literature, the role of the atmosphere in the long-range transportation of microplastics (MPs) has been highlighted (Allen et al., 2019; Liu et al., 2020; Roblin et al., 2020). Thus, MPs, and in particular fibrous MPs that have relatively high aspect ratios (and surface area–to–volume ratios) and low settling velocities (Brahney et al., 2020; Wright et al., 2020), can be transported 100s or 1000s of km from their point of origin before undergoing dry or wet deposition (Liu et al., 2019; Abbasi and Turner, 2021; González-Pleiter et al., 2021). Because of their small size and persistence, MPs in the atmosphere are a concern from a human health perspective (Prata, 2018),

while their deposition in soils, lakes and the ocean represents a means by which MP may be moved between ecosystems and exert impacts on a wide range of organisms (Arias-Andres et al., 2019; Sobhani et al., 2021). With dust storms capable of shifting significant quantities of loose soils, and MPs known to be dispersed amongst soils remote from any urban, industrial and agricultural sources (Feng et al., 2020; Abbasi et al., 2021a), it is hypothesized that storm events may act as a vehicle for transporting considerable quantities of fine, resuspendable MP. Accordingly, the present study involves the opportunistic sampling of dust deposited throughout the metropolis of Shiraz, Iran, immediately after a particularly intense dust storm in May 2018. MPs were isolated from the deposited dust particles, and quantified and characterized by established techniques in order to gain an insight into the significance of dust storms in Iran, and more generally, to the global atmospheric dispersion and redistribution of plastics.

2. Methods

2.1. Study area and sample collection

Shiraz is the largest city of Fars province and southwestern Iran, with a population of about 1.6 million contained within an area of 240 km^2 and lying about 1500 m above sea level. The region is arid in summer and rainy and mild in winter, with an annual average temperature and rainfall of 18°C and 337 mm, respectively, and predominantly southeasterly and easterly winds. The air quality of Shiraz has declined over recent years because of the rapid growth in population, traffic volume and industrialization (Gharehchahi et al., 2013), coupled with an increased incidence of dust storms (Alizadeh-Choobari et al., 2015). The frequency of dust "events" in Shiraz appears to be between 1 and 3% (Alizadeh-Choobari et al., 2015) but on May 13th 2018, a particularly intense

dust storm occurred in the region that involved the transboundary transportation of geogenic material originating in Saudi Arabia across the Persian Gulf (Abbasi et al., 2021b).

Settled dust particles from the storm were collected opportunistically from parked cars, an approach adopted by Bergmann et al. (2019) for the sampling of MPs in fresh European snow. Twenty-two locations (encompassing urban, residential and commercial areas) within different municipal sectors of Shiraz (Figure 1 and Table 1) were visited within six hours after the dust storm by three operators, and five to ten cars at each location were selected from bays with restricted (i.e., not long-term) parking. Sampling involved the careful but rapid retrieval of material from the central regions (about 40 x 40 cm) of windscreens or back windows using a pre-cleaned wooden brush with horsehair bristles and a stainless steel dustpan by an operator wearing cotton clothing. Composite samples from each location were stored in 300 mL glass jars and the brush and pan were washed several times with filtered water between sampling locations. The general atmospheric conditions in Shiraz at this time of year require car windows to be regularly cleaned while driving and we assume, therefore, that the majority of material collected from the windows arose largely from the storm and not from more general, ambient urban deposition.

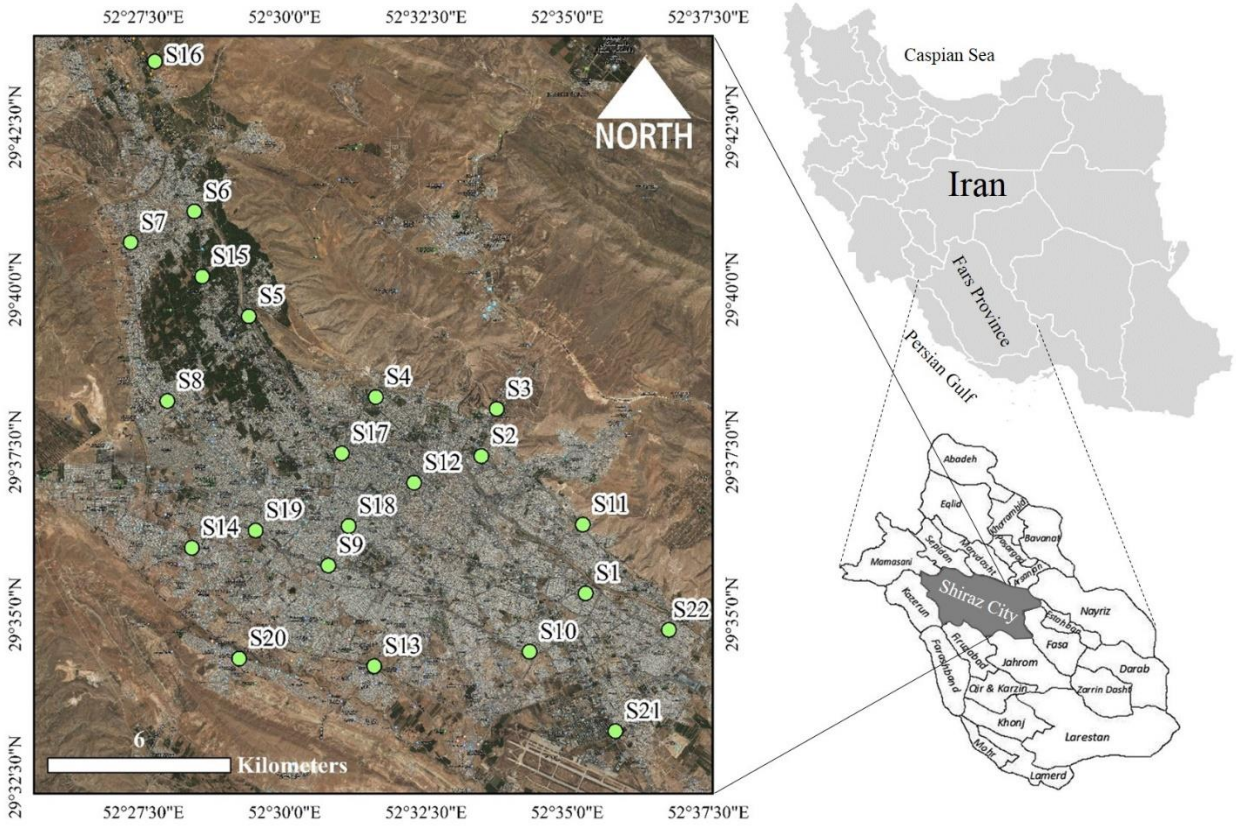

Figure 1: Sampling locations within the metropolis of Shiraz, southwest Iran.

2.2. Sample treatment and microplastic extraction

Dust samples were transferred to individual, 600-mL glass beakers using a stainless steel spoon before being dried for 24 h at 25°C. Dried samples were then sieved through a 5-mm stainless steel mesh, with 50 g of each weighed into individual clean beakers on a Libror AEL-40SM balance (Shimadzu, Kyoto). The contents of each beaker were oxidized with 200-300 mL of 35% H_2O_2 (Arman Sina, Tehran) at room temperature until bubble formation ceased. Remaining particulate matter was washed with filtered, deionized water through a 150 mm diameter S&S filter paper (blue band, grade 589/3, 2 µm pore size) housed in a glass-ceramic vacuum filtration kit before being dried in a sand bath at 60°C for 2 h.

To isolate MPs, each dried, digested sample was transferred to a saturated 300 mL solution of $ZnCl_2$ (Arman Sina, Tehran; density 1.6 – 1.8 g cm^{-3}) in a series of clean glass beakers, and the decanted contents were subsequently centrifuged at 4000 rpm before supernatants were vacuum-filtered through S&S filter papers. This process was repeated twice, with resulting filters air-dried for 48 h at 25 ^{o}C under laminar flow and transferred to glass Petri dishes for physical and chemical characterization.

2.3. Quality assurance and control

Appropriate measures were taken to minimize MP contamination in the laboratory. Thus, benches were cleaned with ethanol using cotton cloths, laboratory clothing was cotton-based and all reagents and solutions were vacuum-filtered through S&S blue band filters (< 2 µm) before being used. All glassware was washed with phosphate-free soap, double rinsed with filtered (< 2 µm) water and soaked in 10% Merck Suprapur HNO_3 for 24 h before being rinsed twice with double-distilled water and air-dried at room temperature in a clean room. Where possible, containers were protected by covering or wrapping in aluminium foil. Controls, consisting of empty beakers that were processed as above, revealed no detectable airborne MP contamination throughout sample processing and storage.

2.4. Microplastic identification

MPs on filters were identified and quantified according to thickness and cross sectional properties, shininess, hardness, surface structure and reaction to a hot, 250 µm stainless steel needle under a binocular microscope (Carl-Zeiss) at up to 200 x magnification and with the aid of ImageJ software. Particle size, with a lower limit of about 20 to 50 µm depending on shape and colour,

156 was estimated along the length of the longest axis, L ($L \leq 100$ µm, $100 < L \leq 250$ µm, $250 \leq L <$
157 500 µm, $500 \leq L < 1000$ µm, $L \geq 1000$ µm), and colour was grouped as black-grey, yellow-orange,
158 white-transparent, red-pink or blue-green. Shape was classified as film, fragment, spherule-granule
159 or fibre, with the latter defined as having a length to diameter ratio of at least three and diameter
160 estimated to the nearest 5 µm with the aid of TCapture software.

161 The polymeric composition of a selection of MPs from different locations and of different colours,
162 sizes and shapes (n = 39) was determined using a micro-Raman spectrometer (LabRAM HR,
163 Horiba, Japan) with a laser of 785 nm, a Raman shift of 400-1800 cm^{-1} and acquisition times
164 between 20 and 30 s. Surface morphology was determined on 21 of these samples, after they had
165 been mounted on microscope slides and gold-coated, using a high vacuum scanning electron
166 microscope (SEM; TESCAN Vega 3, Czech Republic) operated with a resolution of 2 nm at 20
167 kV and equipped with an energy-dispersive X-ray microanalyzer (EDX).
168
169 ***2.5. Trajectory calculations***
170 The origins of air masses and potential source range of material from the dust storm was evaluated
171 from 48-h back trajectories for 13th May 2018, calculated using the National Oceanic and
172 Atmospheric Administration online software, Hybrid Single Particle Lagrangian Integrated
173 Trajectory (HYSPLIT) *v*4, and Global Forecast System (0.25 degree global) meteorological data.
174 Trajectories were calculated at six-hour intervals at a height of 500 m above ground level and a
175 resolution of 1 degree, and were integrated as frequency distributions.
176
177 **3. Results and Discussion**
178 ***3.1. Distribution and characteristics of microplastics***

179 The number and distribution (by size and shape) of the MP identified in the present study are
180 shown for each location sampled in Table 1. Overall, 485 MP were recorded that were dominated
181 by fibres (n = 448 or ~ 92%). Small contributions arose from films (n = 35) and fragments (n = 2)
182 but more regular spherules-granules were never detected. Regarding MP colour, > 50% were
183 white-transparent, 23% were red-pink, 10% were black-grey or yellow-orange, and < 5% were
184 blue-green; non-fibrous MP were dominated (~ 90%) by white-transparent films. The total number
185 of MP at each location ranged from 2 to 53, with concentrations on a number basis ranging from
186 0.04 to 1.06 MP per g of dust. Overall, mean and median concentrations were 0.44 and 0.31 MP
187 g^{-1}, respectively, and 25th and 75th percentiles were 0.21 and 0.65 MP g^{-1}, respectively.

188 Fibres were single straight, curled or coiled strands or, occasionally, multiple, intertwined strands,
189 and diameters ranged from about 10 to 40 μm and averaged 18.7 μm. Over 60% of fibres were
190 encountered in the smallest length category considered (≤ 100 μm), with a similar distribution
191 among size categories up to 1000 μm (10 to 15%) but < 0.5% of fibres present above 1000 μm.
192 The percentage in the finest fraction is subject to some uncertainty because of the existence of MPs
193 below our size detection limit and the possibility that some larger fibres may fragment into smaller
194 particles during centrifugation. Nevertheless, the percentage of fibres in this fraction is larger than
195 that reported for deposited dust particles sampled in Shiraz throughout the year (average ~ 30%)
196 that had been processed and identified using the same methodology (Abbasi and Turner, 2021).
197 Based on a range of aspect ratios (β) from 3 to 100, diameters (d) as above and densities (ρ) for
198 the polymers shown in Figure 2 (from 1.0 to 1.4 g cm^{-3}), we estimate aerodynamic equivalent
199 diameters (d_a) from the following equation (Wright et al., 2020):

200 $$d_a = (\rho \ln 2 \beta)^{1/2} d \qquad (1)$$

to range from about 13 to 130 μm for the fibres detected in the present study.

Table 1: Location of each sampling station in Shiraz (see Figure 1), along with a summary of the MP distribution by size and shape. Fibres are categorised according to length, *L*, but other (remaining) MPs are not classified by shape or size. Concentration represents the number of MP per g of dust.

Sample	UTM coordinates		MP fibres (*L* , μm)					Other MPs		
location	X	Y	< 100	100≤*L* <250	250≤*L* <500	500≤*L* <1000	≥1000	All sizes	Total	Concentration, MP g^{-1}
1	653872	3274271	28	0	0	0	2	0	30	0.60
2	650842	3278127	22	8	1	5	0	1	37	0.74
3	651261	3279474	10	3	10	4	0	0	27	0.54
4	647803	3279769	10	0	0	0	0	0	10	0.20
5	644147	3282014	0	0	0	35	0	3	38	0.76
6	642555	3284973	11	2	0	0	0	2	15	0.30
7	640747	3284072	13	0	0	0	0	0	13	0.26
8	641853	3279579	28	17	0	0	0	2	47	0.94
9	646509	3274962	9	3	0	0	0	0	12	0.24
10	652295	3272590	2	0	0	0	0	0	2	0.04
11	653768	3276225	9	0	0	0	0	0	9	0.18
12	648930	3277346	8	0	0	0	0	0	8	0.16
13	647860	3272117	3	2	4	0	0	3	12	0.24
14	642604	3275416	5	0	11	0	0	0	16	0.32
15	642800	3283128	12	0	28	1	0	6	47	0.94
16	641370	3289215	11	0	0	0	0	0	11	0.22
17	646854	3278154	7	0	0	0	0	0	7	0.14
18	647076	3276095	0	2	13	0	0	8	23	0.46
19	644418	3275928	23	0	0	0	0	10	33	0.66
20	643999	3272283	50	3	0	0	0	0	53	1.06
21	654777	3270363	5	0	0	0	0	0	5	0.10
22	656267	3273264	15	13	0	0	0	2	30	0.60
total			281	53	67	45	2	37	485	
mean			12.8	2.4	3.0	2.0	0.1	1.7	22.0	0.44
min			0	0	0	0	0	0	2	0.04
max			50	17	28	35	2	10	53	1.06

The distribution of selected MPs (n = 39) from various locations by polymer type is shown in Figure 2, along with examples of Raman spectra for two fibres. About one half of the samples were constructed of nylon, with decreasing contributions from polypropylene, polyethylene terephthalate and polystyrene. Fibres (n = 31) were represented by all polymer types detected and reflect the nature of plastics used in textiles and fabrics (Henry et al., 2019), but films (n = 6) were constructed of only nylon and polypropylene and fragments (n = 2) were constructed of nylon.

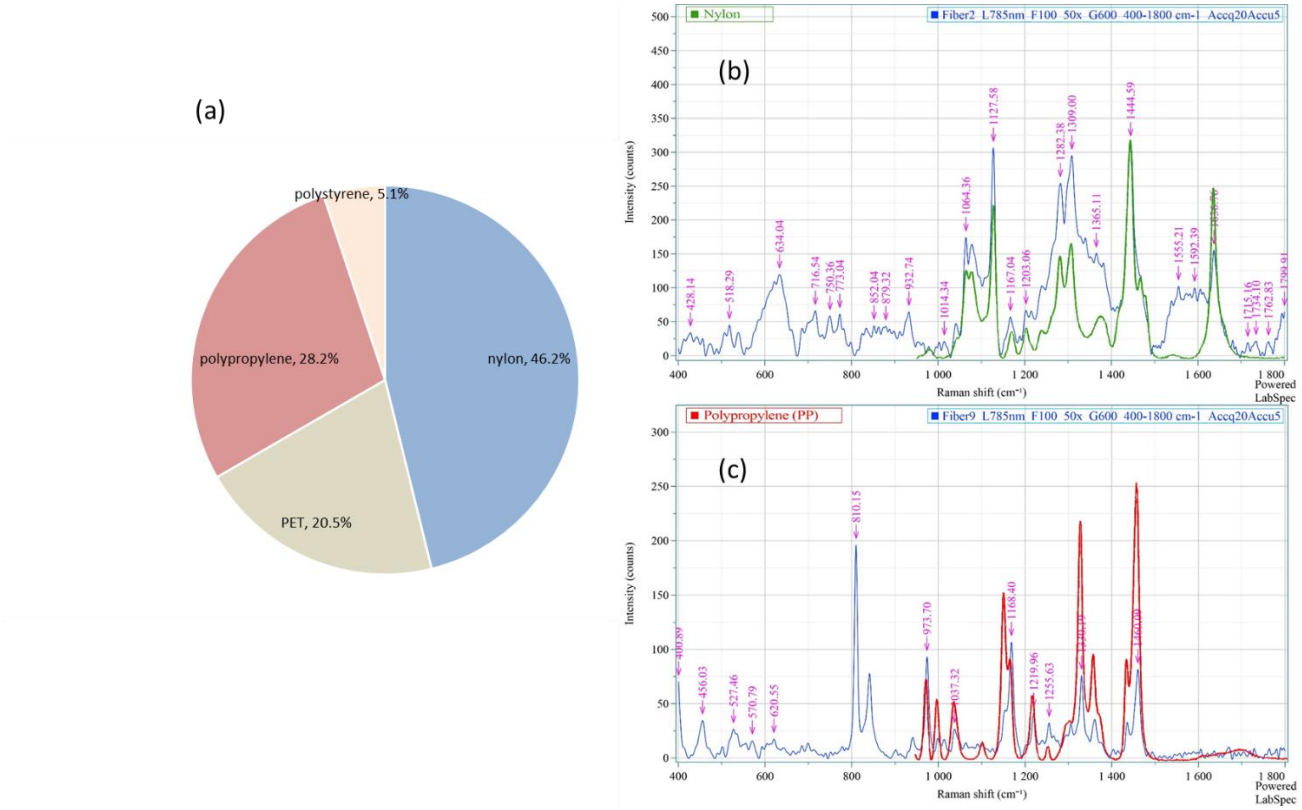

Figure 2: (a) Relative abundance of 39 MPs by polymer type (PET = polyethylene terephthalate), and Raman spectra for (b) a nylon fibre and (c) a polypropylene fibre.

SEM images of selected fibres and films are illustrated in Figure 3. Fibres are uniform in diameter, with the scale bars confirming that sample diameters ranged from about 10 to 40 μm. The images suggest varying degrees of weathering and contamination by adherent mineral particles, with EDX spectra of the latter (and in particular Al, Ca, Mg, Fe, Si and Ti) consistent with the geochemical signature of soils and lithological units in Saudi Arabia and southwest Iran (Abbasi et al., 2021b). Specifically, the fibres shown in Figures 3a and 3b exhibit smooth surfaces with very little evidence of weathering but contamination by extraneous material apparent in the latter case, while the fibres shown in Figures 3c and 3d exhibit contamination and considerable but heterogeneous

227 weathering. In Figure 3c, indentations and pits are indicators of mechanical weathering while
228 flaking and granulation are more typical of photo-oxidation (Zbyszewski and Corcoran, 2011). In
229 Figure 3d, we suspect that the almost parallel but irregular, circular fractures normal to the length
230 of fibre result from shrinkage-expansion while exposed to extreme environmental temperatures.
231 The plastic films illustrated in Figures 3e and 3f contrast the effects of intense photo-oxidation
232 (granulation and flaking) and mechanical weathering (grooves and indentations) on the surface
233 morphologies of thin, angular plastic films.

234

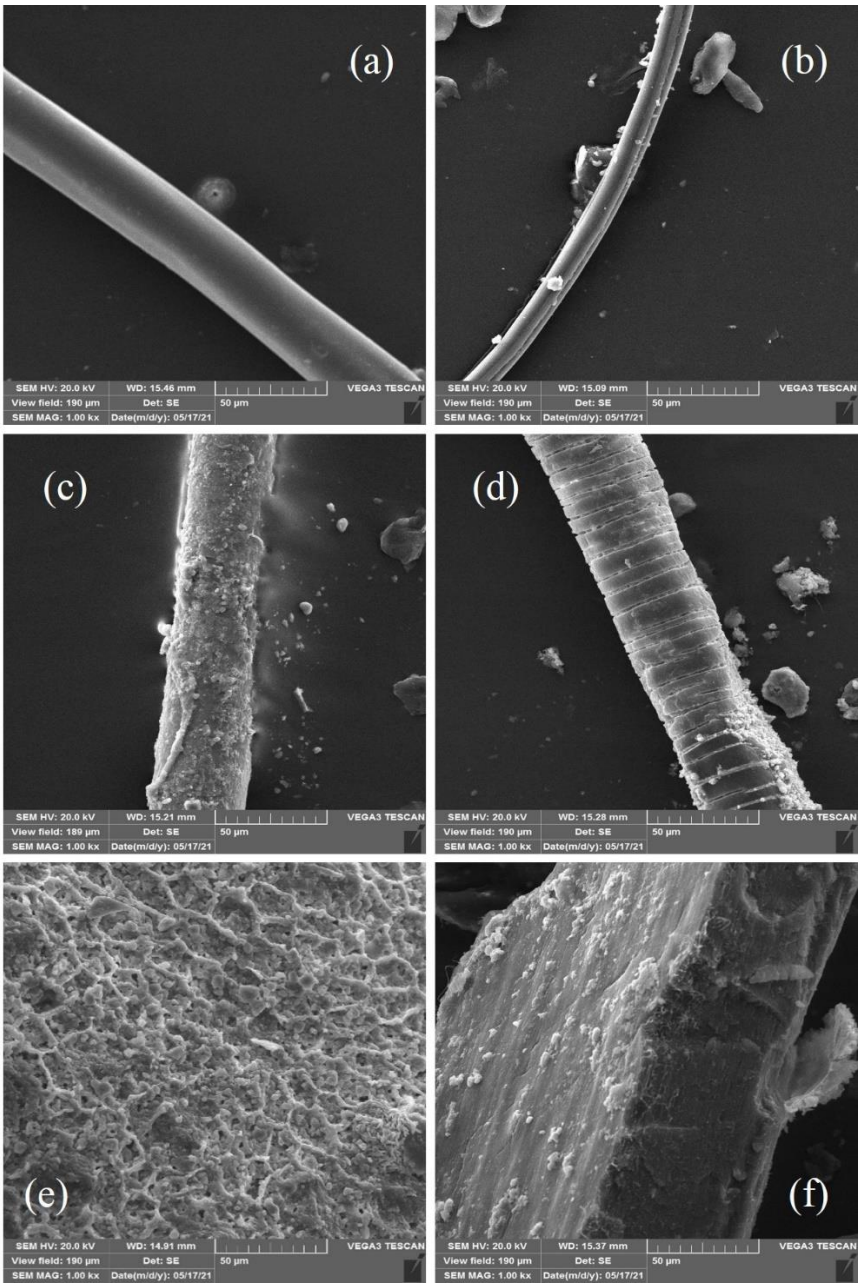

Figure 3: SEM images of six MP retrieved from material deposited in Shiraz after the dust storm. (a) Green polypropylene fibre, (b) red polypropylene fibre, (c) white polyethylene terephthalate fibre, (d) green polypropylene fibre, (e) colourless polypropylene film, (f) purple nylon film.

3.2. Origin of dust and microplastics

The air mass trajectory frequencies for the period directly preceding the dust storm and calculated using HYSPLIT are shown in Figure 4a. These frequencies indicate dominant westerly and southwesterly components associated with the event, with satellite imagery (Figure 4b) and geochemical signatures reported in Abbasi et al. (2021b) confirming that the most important source of dust is the Arabian Peninsula, and in particular the Saudi Arabian deserts. Here, resuspension of material is favoured by extensive accumulations of fine sand and silt, scattered vegetation and variable terrain (Engelbrecht et al., 2017).

The MPs deposited in Shiraz following the dust storm may, therefore, have both distant (or remote) and more local origins. Distant MPs are carried by strong winds with geogenic material (e.g., silicates, aluminosilicates, carbonates) from the Arabian Peninsula, and may be augmented by entrainment of additional plastics in southwest Iran and, potentially, through breaking waves at sea (Allen et al., 2020) as air moves across the Persian Gulf. Local MPs are resuspended with natural soils (mainly silt and clay) and anthropogenic particulates within the urbanized region of Shiraz as the dust storm passes through the metropolis. Nematollahi et al. (2021) found a clear linear correlation between $\delta^{18}O$ and $\delta^{13}C$ isotopes measured in deposited dust particles in Shiraz arising from the dust storm reported here that was attributed to the mixing of two particle end-members: namely, an “anthropogenic” population and a less contaminated but more “geogenic” population. Likewise, it is proposed that MPs in deposited dust particles in Shiraz following the dust storm are derived from and can be modelled by two end-member mixing.

3.3. End-member microplastic mixing model

In the present context, the end-members of MPs observed at a location impacted by a dust storm can be defined as those associated with geogenic material that are imported by the atmosphere with strong winds, and those already resident at the location but suspended by the event itself (and including any material sampled from car windows that was present before the dust storm). The two populations of MP may be different because of distinctly different sources, histories and ages, but are more likely to exhibit some similarities because of the global reach of plastic products and common means of generating MP, coupled with the mixing effects of previous dust events at the location of interest. Without characterizing the end-members themselves, it is not possible to establish any clear differences in these populations. However, SEM observations suggest that MPs imported form the Arabian deserts could exhibit distinctive weathering patterns (such as the shrinkage observed in Figure 3d), while a greater proportion of smaller, fibrous MPs observed in the present study compared with MPs in settled dust particles of Shiraz suggests that imported particles are relatively fine. Conversely, more general aerodynamic considerations and observations in the literature suggest that more rapidly settling, larger fibres and non-fibrous particles are likely to have a local origin (Brahney et al., 2020; Loppi et al., 2021). Nevertheless, and regardless of these characteristics, binary mixing can be considered numerically from MP concentrations representative of the end-member populations.

Thus, typical concentrations of MPs on a number basis in background settled urban dust particles from Shiraz are about 25 MP g^{-1} (Abbasi and Turner, 2021), which is similar to the median concentration of MP measured in street dusts from the industrialized city of Asaluyeh, western Iran (about 15 MP g^{-1}; Abbasi et al., 2019), while concentrations in desert soils remote from any urbanization and derived from the dispersion of distal sources average about 0.02 MP g^{-1} (Abbasi

et al., 2021a). Assuming that dust and MPs exhibit similar entrainments into the atmosphere, the fractional contribution, *f*, of each end-member to the net concentration of MP observed in the dust storm, $[MP]_{dust}$, can be modelled as follows:

$$[MP]_{dust} = f_{rem}[MP]_{rem} + f_{loc}[MP]_{loc} \quad (2)$$

where subscripts rem and loc refer to remote and local sources, respectively. Substituting $1-f_{loc}$ for f_{rem}:

$$[MP]_{dust} = [MP]_{rem} - f_{loc}[MP]_{rem} + f_{loc}[MP]_{loc} \quad (3)$$

and rearranging yields:

$$f_{loc} = ([MP]_{dust}-[MP]_{rem})/([MP]_{loc}-[MP]_{rem}) \quad (4)$$

Using the typical or average end-member MP concentrations above for $[MP]_{loc}$ and $[MP]_{rem}$ of 20 and 0.02 MP g^{-1}, respectively, and the median MP concentration in Table 1 as $[MP]_{dust}$ (0.31 MP g^{-1}) results in a value of f_{loc} of 0.015; using the lowest and highest MP concentrations in Table 1 for $[MP]_{dust}$ (0.04 and 1.06 MP g^{-1}, respectively) results in values of about 0.001 and 0.05, respectively. Thus, the estimated range in contributions of MP that are local to Shiraz to the sampled dust particles is about 0.1 to 5%, with variations amongst the locations presumably reflecting differences in the proximity to or mobility of urban sources but displaying no clear relationship with particle characteristics (e.g., size, colour or shape). The majority of MP are, however, clearly imported from outside the region (and via Saudi Arabia and southwest Iran), with geochemical analyses of dust samples suggesting that the Arabian Peninsula provides the more significant, transboundary contribution (Abbasi et al., 2021b).

3.4. Wider implications

The numerical estimates of MP origin are subject to various assumptions, including processes involved in the suspension-transport-deposition that are similar for both geogenic material and MPs. Nevertheless, they highlight the importance of dust events to the redistribution of MP in arid and semi-arid regions and add to the growing body of evidence in the literature supporting the more general long-range and transboundary atmospheric transport of fibrous MP (Allen et al., 2019; Brahney et al., 2020; Evangeliou et al., 2020).

Although the mass of mobile dust involved in the storm under study does not appear to have been estimated, an earlier event occurring in the Arabian Peninsula and simulated by Jish Prakash et al. (2015) suggested that nearly 100 Mt of dust was emitted, with 73 Mt deposited over the broader region of study and including about 7 Mt deposited in the ocean. Assuming that the concentration of MP in the soils acting as a source of dust is about 0.02 MP g^{-1} (Abbasi et al., 2021b), we estimate that such a storm could suspend about 2 x 10^{12} MP and deposit 1.5 x 10^{12} MP regionally, including 1.5 x 10^{11} MP in the ocean. Globally, it is estimated that about 2 billion tonnes of loose and poorly vegetated arid soil are transported in the atmosphere each year (Perkins, 2001; Tanaka and Chiba, 2006), with the main source regions associated with the Sahara desert and the deserts of Asia, the Middle East, North and South America and Australia (Wang, 2015). Assuming that the soil concentration of MPs employed in the present study is more generally applicable, dust storms could be responsible for the annual, atmospheric mobilization and transportation of about 4 x 10^{13} MP. For representative fibrous MPs of unit density and 250 μm in length and 10 μm in diameter, this is equivalent to about a tonne of MPs. Dust storms, therefore, represents a significant means

by which MPs are redistributed in the environment and, given the proximity of many dust sources to the coastal zone, a potentially important, indirect source of MPs to the ocean. Moreover, with the intensity and frequency of droughts predicted to increase (Srivasta et al., 2018), along with increasing demands for water (Hoff, 2009) and plastic (Geyer et al., 2017), dust storms are likely to be of increasing importance to the global flux and cycling of environmental MPs.

The current study is also significant in highlighting the presence of a type of contaminant suspended in dust storms that has thus far been overlooked. The precise health impacts of airborne MPs, and in particular those that are inhalable, are unclear (Wright et al., 2019; Rahman et al., 2021), but any effects associated with dust storms should be considered along with those arising from the presence of other materials and chemicals, including dust itself, allergenic particles, like pollen and fungi, microbiological organisms, and heavy metals (Kellogg and Griffin, 2006).

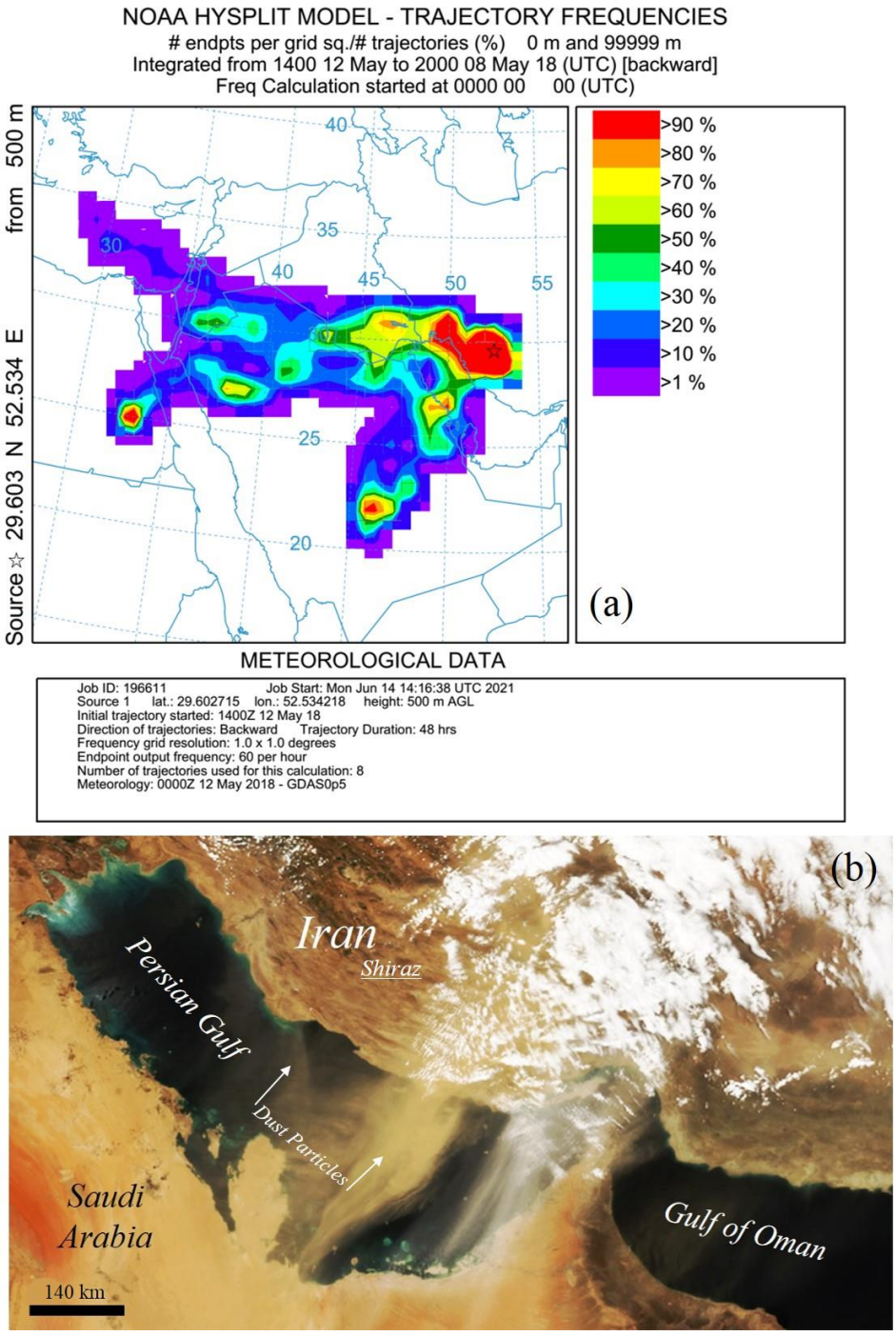

Figure 4: (a) Frequencies of air trajectories crossing a given area and arriving at Shiraz (starred) for 8th to 12th May 2018 calculated at 500 m and from 48 h air mass back-trajectories using HYSPLIT, and (b) NOAA satellite image of the region during the dust storm.

4. Conclusions

This study is the first to document MPs associated with and transported by a dust storm. With respect to an intense event in the metropolis of Shiraz in May 2018, the majority of plastics isolated from deposited dust particles were fibrous, with concentrations on a number basis ranging from < 0.05 to about 1.1 MP g^{-1}. MPs exhibited varying degrees of mechanical weathering, photo-oxidation and contamination by geogenic particulates, and the provenance of the latter, coupled with satellite imagery and HYSPLIT modelling, suggests that the majority of material brought into Shiraz originates from the Saudi Arabian Peninsula. Within the uncertainties and assumption of a two end-member MP mixing model, we estimate that > 90% of plastics in deposited dusts are derived from outside the city. Globally, dust storms could represent a significant means of MP transportation in the atmosphere and an important source of MPs to the ocean.

Acknowledgments

We thank Shiraz University for supporting this study (grant number: 99GRC1M371631). The comments of anonymous reviewers are greatly appreciated.

References

Abbasi, S., Turner, A., 2021. Dry and wet deposition of microplastics in a semi-arid region (Shiraz, Iran). Science of the Total Environment 786, 147358.

Abbasi, S., Keshavarzi, B., Moore, F., Turner, A., Kelly, F.J., Dominguez, A.O., Jaafarzadeh, N., 2019. Distribution and potential health impacts of microplastics and microrubbers in air and street dusts from Asaluyeh County, Iran. Environmental Pollution 244, 153-164.

Abbasi, S., Turner, A., Hoseini, M., Amiri, H., 2021a. Microplastics in the Lut and Kavir Deserts, Iran. Environmental Science and Technology 55, 5993-6000.

Abbasi, S., Rezaei, M., Keshavarzi, B., Mina, M., Ritsema, C., Geissen, V., 2021b. Investigation of the 2018 Shiraz dust event: Potential sources of metals, rare earth elements, and radionuclides; health assessment. Chemosphere 279, 130533.

Alizadeh-Choobari, Ghafarian, P., Owlad, E., 2015. Temporal variations in the frequency and concentration of dust events over Iran based on surface observations. International Journal of Climatology 36, 2050-2062.

Allen, S., Allen, D., Phoenix, V.R., Le Roux, G., Jimenez, P.D., Simonneau, A., Binet, S., Galop, D., 2019. Atmospheric transport and deposition of microplastics in a remote mountain catchment. Nature Geoscience 12, 339-344.

Allen, S., Allen, D.,Moss, K., Le Roux, G., Phoenix, V.R., Sonke, J.E., 2020. Examination of the ocean as a source for atmospheric microplastics. PLoS ONE 15, e0232746.

Arias-Andres, M., Rojas-Jimenez, K., Grossart, H.P., 2019. Collateral effects of microplastic pollution on aquatic microorganisms: An ecological perspective. Trends in Analytical Chemistry 112, 234-240.

Behrooz, R.D., Kaskaoutis, D.G., Grivas, G., Mihalopoulos, N., 2020. Human health risk assessment for toxic elements in the extreme ambient dust conditions observed in Sistan, Iran. Chemosphere 262, 127835.

Brahney, J., Hallerud, M., Heim, E., Hahnenberger, M., Sukumaran, S., 2020. Plastic rain in protected areas of the United States. Science 368, 1257-1260.

Engelbrecht, J., Stenchikov, G.L., Prakash, P.J., Lersch, T., Anisimov, A. and Shevchenko, I., 2017. Physical and chemical properties of deposited airborne particulates over the Arabian Red Sea coastal plain. Atmos. Chem. Phys., 17, p.11467–11490, https://doi.org/10.5194/acp-17-11467-2017.

Evangeliou, N., Grythe, H., Klimont, Z., Heyes, C., Eckhardt, S., Lopez-Aparicio, S., and Stohl, A., 2020. Atmospheric transport is a major pathway of microplastics to remote regions. Nature Communications 11, 1–11.

Feng, S.S., Lu, H.W. Tian, P.P., Xue, Y.X., Lu, J.Z., Tang, M., Feng, W., 2020. Analysis of microplastics in a remote region of the Tibetan Plateau: Implications for natural environmental response to human activities. Science of the Total Environment 739, 140087.

Gharehchahi, E., Mahvi, A.H., Amini, H., Nabizadeh, R., Akhlaghi, A.A., Shamsipour, M., Yunesian, M., 2013. Health impact assessment of air pollution in Shiraz, Iran: a two-part study. Journal of Environmental Health Sciences & Engineering 11, 11.

Geyer, R., Jambeck, J.R., Law, K.L., 2017. Production, use, and fate of all plastics ever made. Science Advances 3, e1700782.

González-Pleiter, M., Edo, C., Aguilera, A., Viúdez-Moreiras, D., Pulido-Reyes, G., González-Toril, E., Osuna, S., de Diego-Castilla, G., Leganés, F., Fernández-Piñas, F., Rosal, R., 2021. Occurrence and transport of microplastics sampled within and above the planetary boundary layer. Science of the Total Environment 761, 143213.

Goudie, A.S., 2009. Dust storms: Recent developments. Journal of Environmental Management 90, 89-94.

Henry, B., Laitala, K., Klepp, I.G., 2019. Microfibres from apparel and home textiles: Prospects for including microplastics in environmental sustainability assessment. Science of the Total Environment 652, 483-494.

Hoff, H., 2009. Global water resources and their management. Current Opinion in Environmental Sustainability 1, 141-147.

Jish Prakash, P., Stenchikov, G., Kalenderski, S., Osipov, S., Bangalath, H., 2015. The impact of dust storms on the Arabian Peninsula and the Red Sea. Atmospheric Chemistry and Physics 15, 1990222.

Kellogg, C.A., Griffin, D.W., 2006. Aerobiology and the global transport of desert dust. Trends in Ecology and Evolution 21, 638-644.

Liu, K., Wu, T., Wang, X., Song, Z., Zong, C., Wei, N., Li, D., 2019. Consistent transport of terrestrial microplastics to the ocean through atmosphere. Environmental Science and Technology 53, 10612-10619.

Liu, K., Wang, X., Song, Z., Wei, N., Haoda, Y., Cong, X., Zhao, L., Li, Y., Qu, L., Zhu, L., Zhang, F., Zong, C., Jiang, C., Li, D., 2020. Global inventory of atmospheric fibrous microplastics input into the ocean: An implication from the indoor origin. Journal of Hazardous Materials 400, 123223.

Loppi, S., Roblin, B., Paoli, L., Aherne, J., 2021. Accumulation of airborne microplastics in lichens from a landfill dumping site (Italy). Scientific Reports 11, 4564.

Nematollahi, M.J., Abbasi, S., Mohammadi, Z., Hopke, P.K., Moravej, S., Swennen, R., Duce, R., Reichman, S.M., 2021. The Shiraz metropolis dust storm event in Iran: A comprehensive investigation (in review).

Ogorodnikov, B.I., 2011. A dust storm over the Ukraine and Belarus territory contaminated by radionuclides after the Chernobyl accident. Russian Meteorology and Hydrology 36, 613-623.

Pauley, P.M., Baker, N.L., Barker, E.H., 1996. An observational study of the “Interstate 5” dust storm case. Bulletin of the American Meteorological Society 77, 693-720.

Perkins, S., 2001. Dust, the thermostat: How tiny airborne particles manipulate global climate. Science News 160, 200–2002.

Prata, J.C., 2018. Airborne microplastics: consequences to human health? Environmental Pollution 234, 115–126.

Rahman, A., Sarkar, A., Yadav, O.P., Achari, G., Slobodnik, J., 2021. Potential human health risks due to environmental exposure to nano-and microplastics and knowledge gaps: A scoping review. Science of the Total Environment 757, 143872.

Rashki, A., Middleton, N.J., Goudie, A.S., 2021. Dust storms in Iran – distribution, causes, frequencies and impacts. Aeolian Research 48, 100655.

444 Roblin, B., Ryan, M., Vreugdenhil, A., Aherne, J., 2020. Ambient atmospheric deposition of
445 anthropogenic microfibers and microplastics on the western periphery of Europe (Ireland).
446 Environmental Science and Technology 54, 11100-11108.

447 Sobhani, Z., Panneerselvan, L., Fang, C., Naidu, R., Megharaj, M., 2021. Chronic and
448 transgenerational effects of polystyrene microplastics at environmentally relevant concentrations
449 in earthworms (*Eisenia fetida*). Environmental Toxicology and Chemistry
450 DOI:10.1002/etc.5072.

451 Soleimani, Z., Teymouri, P., Boloorani, A.D., Mesdaghinia, A., Middleton, N., Griffin, D.W.,
452 2020. An overview of bioaerosol load and health impacts associated with dust storms: A focus
453 on the Middle East. Atmospheric Environment 223, 117187.

454 Srivastava, S., Shamseddini, A., Blade, M.K., Rafisura, K., Sarkar-Swaisgood, M., Ahmed, S.,
455 Kim, S.E., Dispert, I., 2018. Sand and Dust Storms in Asia and the Pacific: Opportunities for
456 Regional Cooperation and Action. United Nations Economic and Social Commission for Asia
457 and the Pacific, Bangkok.

458 Tam, W.W.S., Wong, TW., Wong, A.H.S., Hui, D.S.C., 2012. Effect of dust storm events on
459 daily emergency admissions for respiratory diseases. Respirology 17, 143-148.

460 Tan, S.C., Shi, G.Y., Wang, H., 2012. Long-range transport of spring dust storms in Inner
461 Mongolia and impact on the China seas. Atmospheric Environment 46, 299-308.

462 Tanaka, T.Y., Chiba, M., 2006. A numerical study of the contributions of dust source regions to
463 the global dust budget. Global and Planetary Change 52, 88-104.

464 van der Does, M., Knippertz, P., Zschenderlein, P., Harrison, R.G., Stuut, J.-B.W., 2018. The
465 mysterious lonmg-range transport of giant mineral dust particles. Science Advances 4, DOI:
466 10.1126/sciadv.aau2768

467 Wang, J.X.L., 2015. Mapping the global dust storm records: Review of dust data sources in
468 supporting modeling/climate study. Current Pollution Reports 1, 82-94.

469 Wright, S.L., Levermore, J.M., Kelly, F.J., 2019. Raman spectral imaging for the detection of
470 inhalable microplastics in ambient particulate matter samples. Environmental Science and
471 Technology 53, 8947-8956.

472 Wright, S.L., Ulke, J., Font, A., Chan, K.L.A., Kelly, F.J., 2020. Atmospheric microplastic
473 deposition in an urban environment and an evaluation of transport. Environment International
474 136, 105411.

475 Zbyszewski, M., Corcoran, P.L., 2011. Distribution and degradation of fresh water plastic
476 particles along the beaches of Lake Huron, Canada. Water, Air and Soil Pollution 220, 365-372.